Appl. Phys. A (2016) 122:715
DOI 10.1007/s00339-016-0247-9

Applied Physics A
Materials Science & Processing

Non-instantaneous growth characteristics of martensitic transformation in high Cr ferritic creep-resistant steel

Chenxi Liu[1] · Yi Shao[1] · Jianguo Chen[1] · Yongchang Liu[1]

Received: 29 March 2016 / Accepted: 28 June 2016 / Published online: 5 July 2016

Abstract Microstructural observation and high-resolution dilatometry were employed to investigate kinetics of martensitic transformation in high Cr ferritic creep-resistant steel upon different quenching/cooling rates. By incorporating the classical athermal nucleation and impingement correction, a non-instantaneous growth model for martensitic transformation has been developed. The developed model describes austenite/martensite interface mobility during martensite growth. The growth rate of martensite is found to be varied from 1×10^{-6} to 3×10^{-6} m/s. The low interface mobility suggests that it is not appropriate to presume the instantaneous growth behavior of martensite. Moreover, based on the proposed model, nucleation rate of martensite under different cooling rates is found to be nearly the same, while the growth rate of martensite is promoted by increasing the cooling rate.

1 Introduction

High Cr ferritic creep-resistant steels have been the important structural materials for elevated temperature application in fossil-fired power plants, due to their good high-temperature endurance, creep resistance properties, excellent heat conductivity, low thermal expansion coefficient and high performance–cost ratio [1–4]. In addition, considering their outstanding resistance to radiation-induced void swelling and irradiation embrittlement, the reduced activation high Cr ferritic steels have also been chosen as the potential candidate materials for test blanket modules (TBMs) of International Thermonuclear Experimental Reactor (ITER) [5–7].

Since phase-transformation behaviors of steels have a significant effect on the final microstructure attained, the transformation from austenite to martensite in steels has received considerable attention over the years [8]. As the predominant microstructure of high Cr ferritic creep-resistant steels, martensite formed during continuous cooling after austenization has also been studied extensively [9–12]. However, the model for nucleation and growth of martensite in high Cr ferritic steels is rarely mentioned.

The classical martensitic transformation theory suggests that kinetics of martensitic transformation depends solely on nucleation, since the growth of a martensitic crystal usually occurs rapidly. Koistinen and Marburger [13] proposed an empirical equation (named K–M equation) which describes the volume fraction of residual austenite as a function of temperature below the martensite-start temperature. Magee [14] found that the K–M equation could be derived theoretically from basic principles, based on the assumption that martensitic growth is approximately instantaneous. Actually, many experimental results indicate that the growth rate of martensite can be varied in the range from hundreds of m/s to several μm/s [8, 15–18]. Therefore, the assumption of instantaneous growth of martensite may not be appropriate in some cases.

Aimed at investigating the austenite/martensite interface mobility during martensitic growth, the influence of cooling rate on the kinetics of martensitic transformation in high Cr ferritic creep-resistant steel was studied by microstructural observation and dilatometric analysis. On the basis of the kinetics characteristics of martensitic

✉ Yongchang Liu
licmtju@163.com

[1] State Key Lab of Hydraulic Engineering Simulation and Safety, School of Materials Science and Engineering, Tianjin University, Tianjin 300072, People's Republic of China

transformation, a non-instantaneous growth model for martensitic transformation, incorporating the classic athermal nucleation and impingement correction, was developed.

2 Experiment

The chemical composition of the modified high Cr ferritic steel used in this work is given in Table 1. The steel was melted in a vacuum induction furnace into an ingot of 100 kg. Then, it was hot rolled followed by air cooling, and normalized at 1050 °C. In order to assure a homogenous temperature within the dilatometric specimen, the samples were machined into cylindrical samples with a length of (down to) 4 mm and a diameter of 5 mm for dilatometric measurement.

A Bähr DIL 805A/D high-resolution differential dilatometer was used to record the length changes in the samples during heat treatment. The resolution can be up to about ±0.02 μm. To assure a constant temperature during rapid cooling, the initial length of the used dilatometric specimens was limited to about 4 mm. Two additional thermocouples were spot welded at the end, and the surface of the dilatometric specimen, respectively. The difference in temperature between the values registered by these two thermocouples is less than 2 °C during cooling with a cooling rate of 100 °C/s (6000 °C/min). The samples were heated to 1100 °C for 10 min and then cooled to room temperature at different cooling rates (2000, 4000 and 6000 °C/min). The volume fractions of phases were calculated by applying the lever rule, according to the recorded relative length changes by dilatometric measurement. The detail calculation for lever rule can be referred to [19].

After the dilatometric measurement, the samples were mounted, polished and etched in a solution of hydrochloric acid and ferric chloride. The microstructures were examined by C-35A OLYMPUS Optical Microscope (OM) and JEM-100CX II Transmission Electron Microscopy (TEM). For the TEM observation, small disks (3 mm diameter, 0.3 mm thick) were cut out of the samples and then ground to a final thickness of 0.1 mm using successively finer grades of SiC paper to remove equal amounts of material from both sides of the disks. Disks were electro-polished to electron transparency using an electrolytic double-jet technique. As an electrolyte, a mixed solution of 95 vol% acetic acid and 5 vol% perchloric acid was used.

3 Microstructural observation and dilatometric measurement results

The optical micrographs of the high Cr ferritic steel samples upon different cooling rates are presented in Fig. 1. It can be seen that the microstructures of all samples show the typical morphology of martensitic laths. In addition, there is a small amount of δ-ferrite (about 4 % in volume) in the samples, exhibiting irregular white blocks in the micrographs. The formation of δ-ferrite is related to the high content of ferrite stabilizers such as Cr and W. Figure 2 shows the TEM images of the specimens. The effect of cooling rate on the width of martensitic laths inconspicuous, or says width of martensitic laths is almost constant in spite of the cooling rate.

The dependency of calculated martensitic transformation fraction, *f*, on transformation time of the samples under different cooling rates, is shown in Fig. 3, all exhibiting the smooth S-shaped curve. In our previous study, it has been recognized that relatively low cooling rate may cause the splitting phenomenon of martensitic transformation in high Cr ferritic steel, leading to an inflection point in the phase fraction curves of samples. This is relevant to the concentration gradient caused by the consumption of alloying elements in M_3C formation at low cooling rate, while high cooling rate could retard the precipitation of M_3C particles [20, 21]. Thus, here high cooling rates are adopted, to avoid the influence of M_3C precipitation on the kinetics of martensite transformation. Moreover, this could also avoid the influence of diffusion of interstitial atoms such as C or N on martensite transformation if possible, since the starting temperature for martensitic transformation, M_s, is relatively high in high Cr ferritic steel (all above 380 °C; see Table 2).

Nevertheless, it should be pointed out that high cooling rate would bring out the high interior stress, which would affect the kinetics of martensitic transformation. It is well known that the martensitic transformation is accompanied by volume expansion of the samples. Thus, it can be deduced that the martensitic transformation would bring a compressive stress to the samples. Our recent research reveals that the applied uniaxial compressive stress acts a remarkable effect on the kinetics of martensitic transformation [22]. It was found that the driving force for the martensitic transformation decreases with increasing applied uniaxial compressive stress, which is below the yield limits of the high-temperature austenite phase. In other words, minor compressive stress would hinder the

Table 1 Chemical composition of the experimental high Cr ferritic steel (in wt%)

Element	C	Si	Mn	Cr	Mo	W	V	Nb	N	Co	B	Ti	Al
Content	0.05	0.21	0.44	9.81	0.43	1.73	0.22	0.07	0.02	1.41	0.0045	<0.01	0.014

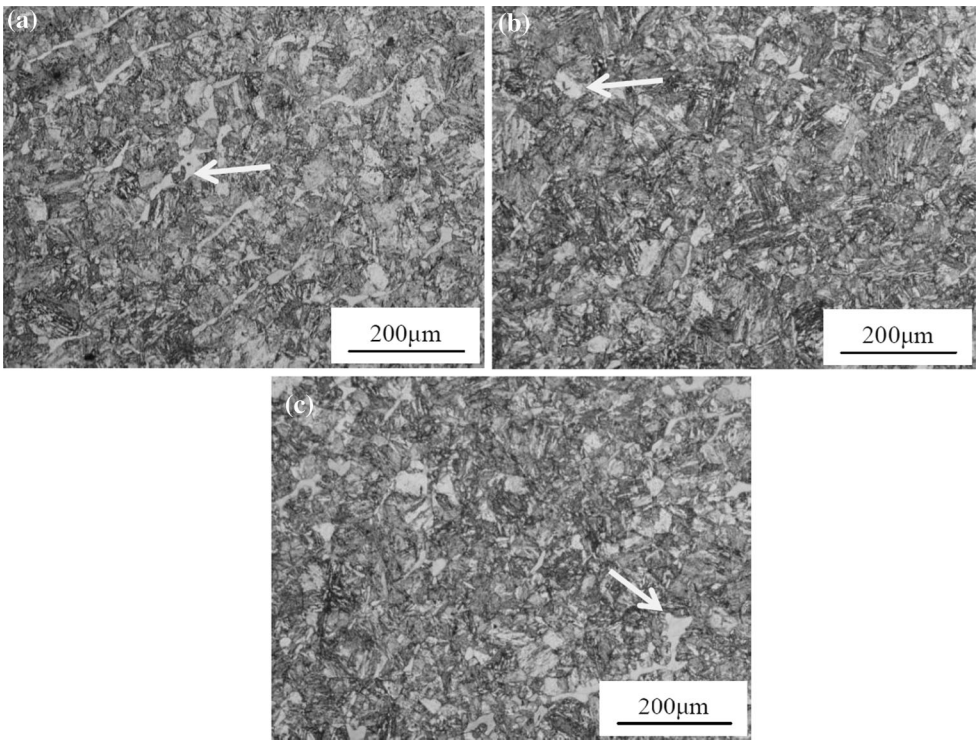

Fig. 1 Optical micrographs of the modified high Cr ferritic steel samples upon different cooling rates: **a** 2000 °C/min; **b** 4000 °C/min; **c** 6000 °C/min

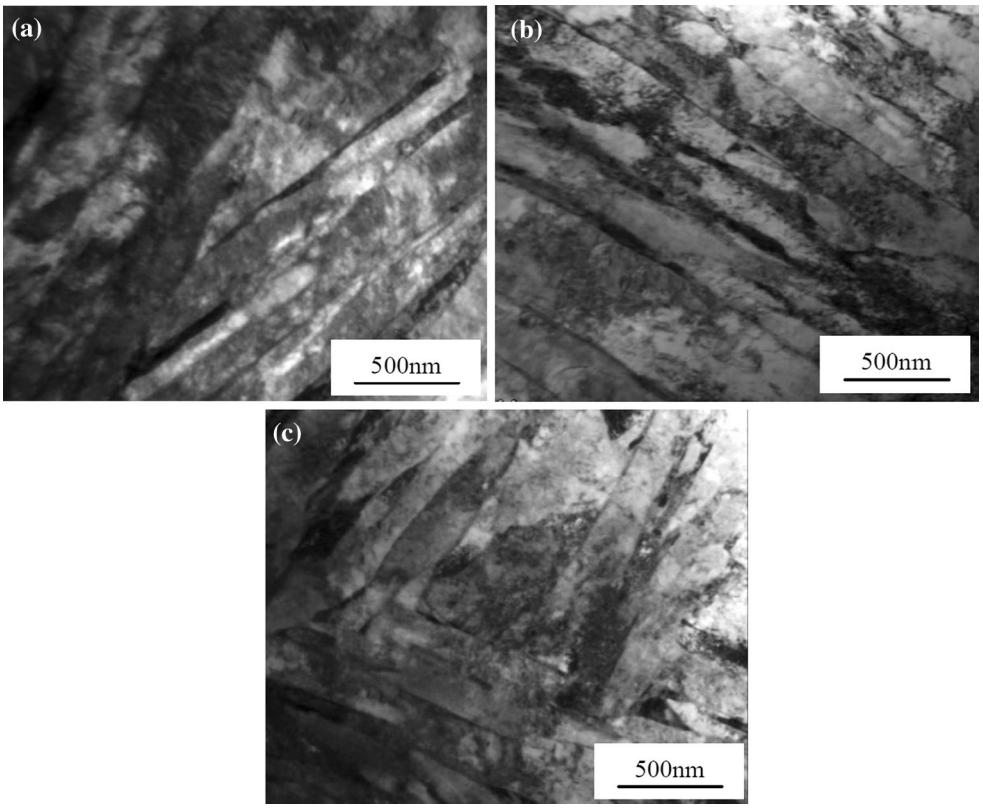

Fig. 2 TEM images of the modified high Cr ferritic steel samples upon different cooling rates: **a** 2000 °C/min; **b** 4000 °C/min; **c** 6000 °C/min

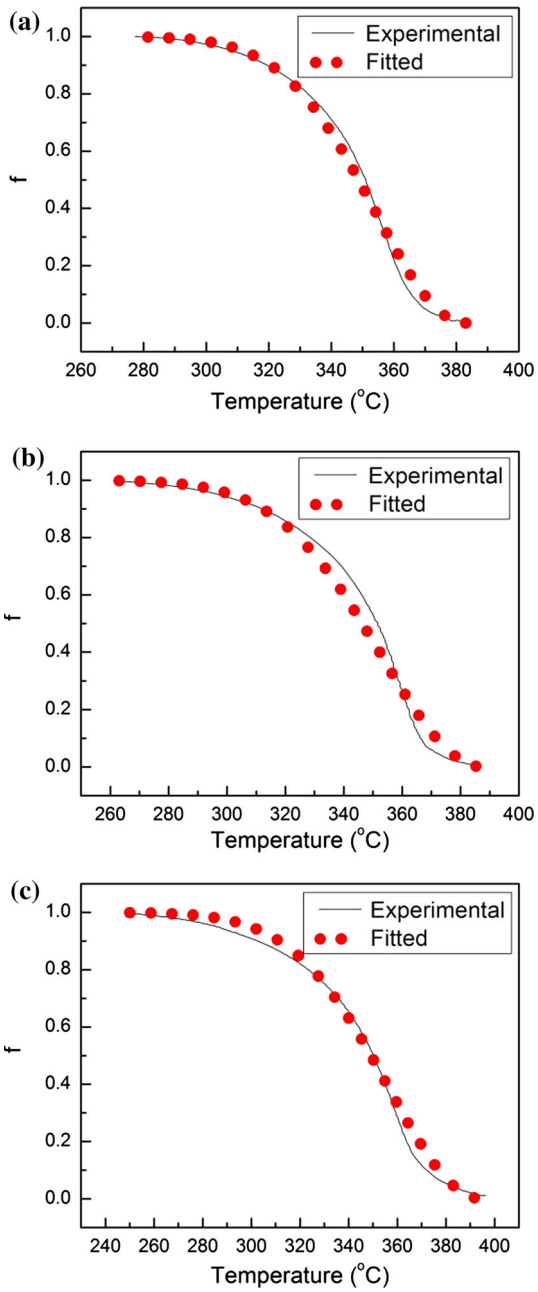

Fig. 3 Martensitic fraction, f, as measured and as fitted by the phase-transformation model (see text) as a function of the transformation temperature for the martensitic transformation of the high Cr ferritic steel samples upon different cooling rates: **a** 2000 °C/min; **b** 4000 °C/min; **c** 6000 °C/min

process of martensitic transformation. Higher cooling rate brings out higher internal stress and thus aggravates this blocking effect. In our previous work, it was also confirmed that the increase of the cooling rate results in increase of temperature range for martensitic transformation [17].

Table 2 Starting temperature for martensitic transformation, M_s, and finishing temperature for martensitic transformation, M_f, determined from the dilatometric measurements

Cooling rate (°C/min)	M_s (°C)	M_f (°C)
2000	383	277
4000	388	261
6000	395	250

4 Non-instantaneous growth model for martensitic transformation

The classical Koistinen–Marburger equation mentioned above has often been used to describe the progress of martensitic transformation upon continuous cooling [13]:

$$f = 1 - \exp(-\beta(M_s - T)) \quad (1)$$

where f is the martensitic fraction, T is absolute temperature, M_s is the starting temperature of martensitic transformation and β is a rate constant dependent on the composition of steel, approximately equaling to 0.011 in steels. This model is based on the assumption of athermal nucleation and instantaneous growth, so that the transformed fraction of martensite only lies on the degree of undercooling, independent of the applied cooling rate [23, 24]. Magee [14] proposed that the K–M equation can be derived from the hypothesis that nucleation rate dN/dT is proportional to the increase in driving force $\Delta G^{\gamma\to\alpha'}$ due to the temperature decrease. Thus, the rate constant β can be expressed as [14]:

$$\beta = \bar{V}\varphi\frac{\mathrm{d}\left(\Delta G^{\gamma\to\alpha'}\right)}{\mathrm{d}T} \quad (2)$$

where $\bar{V}$ is the average volume of martensite unit, $\Delta G^{\gamma\to\alpha'}$ is the difference of martensite and austenite in Gibbs free energy per unit volume, and φ is a constant expressing the proportionality between the increase in driving force and the consequent increase in density of activated nucleation sites. Φ only depends on the chemical composition, austenitizing conditions and applied stress [23, 26]. However, instantaneous growth of crystal seems not reasonable in some sense, no matter how fast the growth rate is. Besides, the kinetics feature that transformed fraction is independent of reaction time may not hold for some materials, at least for the experimental steel employed in this work.

Adopting the classic model for athermal nucleation developed by Magee [14], nucleation rate dN/dT is controlled by the chemical energy difference of martensite and austenite:

$$\frac{dN}{dT} = \varphi \frac{d\left(\Delta G^{\gamma\to\alpha'}\right)}{dT} \tag{3}$$

For the relatively narrow temperature window (e.g., in the temperature span of martensitic transformation), $\frac{d\left(\Delta G^{\gamma\to\alpha'}\right)}{dT}$ can be considered as a constant independence on cooling rate [14, 26]. Therefore, it can be deduced that $\frac{dN}{dT}$ is also a constant. Consequently, by integrating Eq. (3), the martensitic nucleus density at temperature T, $N(T)$, is given as:

$$N(T) = \varphi \frac{d\left(\Delta G^{\gamma\to\alpha'}\right)}{dT}(M_s - T) = \frac{dN}{dT}(M_s - T) \tag{4}$$

where M_s is the martensite starting temperature.

It is well known that the growth rate of martensite is very high (possibly to hundreds of meters per second). Hence, many classic martensitic transformation models is based on the assumption that martensitic growth is approximately instantaneous [14, 23, 27–33]. Fisher–Hollomon–Turnbull model [27] tactfully proposed that the firstly generated martensite sub-grain (namely lath or plate) partitions an initially fully austenite grain. Martensitic sub-grain size gradually decreases, since the volume of partitioned austenite grain gets smaller as the transformation progress. Obviously, this model cannot be applicable to the presented experimental results, since the martensitic lath width is approximately uniform (see Fig. 2). As mentioned above, Magee model [14] based on the classic K–M equation builds the assumption of athermal nucleation and equal grain size, which is more qualified with the present work. Guimarães et al. [32] modeled lath martensite transformation considering autocatalytic nature of martensite, which is also based on the assumption of instantaneous growth of martensite.

In the previous work, the authors have investigated the kinetics of martensite formation in Fe–Al alloys and found that the velocity of austenite/martensite interface during martensitic transformation is about 2×10^{-4} m/s, which is much lower than that in a variety of materials [17]. Further, in multi-composition alloys (such as high Cr ferritic steel used in this project), various types of undissolved or precipitated second particles (as $M_{23}C_6$, MX and M_3C [34]) would hinder mobility of martensitic interfaces and thus decrease growth rate of martensite. Therefore, the growth rate of martensite should not be ignored in the presented work. Nonetheless, length of martensitic lath is far greater than width of that, so the assumptions are reasonable that the lengthening rate of martensitic lath is instantaneous, and the thickening rate of that is equal everywhere. Based on this approximation, the lath is certainly cylindrical in shape, and the volume of one martensitic lath V_M at T can be expressed as:

$$V_M = \frac{1}{4}\pi L^2 \int_{T_\tau}^{T} v\,dT \tag{5}$$

where L is the average length of martensitic lath, T_τ and T are the starting temperature and finishing temperature for lath growth, respectively, v is the average thickening rate of martensitic lath. Consequently, the extended volume of martensite V^e is given as:

$$\begin{aligned} V^e &= \int_{Ms}^{T} V_0 \frac{dN(T)}{dT} V_M dT \\ &= \int_{Ms}^{T} V_0 \frac{dN}{dT}\frac{1}{4}\pi L^2 \left(\int_{T_\tau}^{T} v\,dT\right) dT_\tau \end{aligned} \tag{6}$$

where V_0 is total volume of sample.

The extended volume V^e must be corrected, considered "hard" impingement of the randomly distributed growing particles [35, 36], and the real transformed fraction f can be obtained as:

$$f = 1 - \exp\left(-\frac{V^e}{V_0}\right) = 1 - \exp\left(-\frac{1}{8}\frac{dN}{dT}\pi L^2 v (M_s - T)^2\right) \tag{7}$$

The average length of martensitic lath L can hardly be determined by TEM images, so the value of 10 μm is estimated according to Ref. [37]. Besides, value of nucleation rate dN/dT is difficult to be experimentally obtained. Nevertheless, it can be calculated by Eq. (4):

$$\frac{dN}{dT} = \frac{N(M_f)}{M_s - M_f} \tag{8}$$

where $N(M_f)$ is the martensitic nucleus density at temperature M_f, namely martensitic lath density. Thus, it is easily obtained as:

$$N(M_f) = \frac{1}{\overline{V}} \tag{9}$$

where $\overline{V}$ is the average volume of martensitic lath. According to Eq. (5), $\overline{V}$ can be expressed as:

$$\overline{V} = \frac{1}{4}\pi L^2 W \tag{10}$$

where W is the width of martensitic lath, which is determined by TEM images (see Table 3). Thus, value of martensitic lath density $N(M_f)$ and nucleation rate dN/dT can be determined (see Table 3). $N(M_f)$ is slightly increased with increasing of the cooling rate, due to the decrease in width of martensitic lath. In addition, dN/dT basically remains the same regardless of the cooling rate. As discussed above, dN/dT only depends on $\frac{d\left(\Delta G^{\gamma\to\alpha'}\right)}{dT}$ and φ [see Eq. (3)], both of which depends on the chemical composition of martials and/or austenitizing conditions,

Table 3 Kinetic parameters of the modified high Cr ferritic steel samples upon different cooling rates

Cooling rate (°C/min)	W (m)	$N(M_f)$ (m^{-3})	dN/dT ($°C^{-1}m^{-3}$)	v (m/s)
2000	3.0×10^{-7}	1.42×10^{18}	1.34×10^{16}	1.24×10^{-6}
4000	2.8×10^{-7}	1.62×10^{18}	1.28×10^{16}	1.99×10^{-6}
6000	2.6×10^{-7}	1.88×10^{18}	1.30×10^{16}	2.49×10^{-6}

independent of cooling rate. Hence, the calculated values of dN/dT are consistent with the presented model well.

Combining Eqs. (7), (8), (9) and (10), the fraction of martensite f can be expressed as:

$$f = 1 - \exp\left(-\frac{1}{2}\frac{v(M_s - T)^2}{W(M_s - M_f)}\right) \quad (11)$$

It is found that the fraction of martensite f is irrelevant to the lath length L, which is due to the infinite growth rate of martensite along the lath length assumed in the presented model.

By fitting experimental data to the model, the thickening rate of martensitic lath, v, can be obtained, as listed in Table 3. Figure 3 displays the dependencies of the experimental f and the fitted f on temperature. The experimental results are in well agreement with the predicted values of the model. As can be seen from Table 3, the growth rate of martensite, v, is accelerated by increase in cooling rate. It implies that martensitic transformation is promoted as the cooling rate increases, since the nucleation rate dN/dT is independent of the cooling rate. Comparing with our previous results, the growth rate of martensite in this work is two orders of magnitude smaller than that in Fe-1.0 %Al (at.) alloy [17]. This inconsistency can be explained as follows: (1) High strength of the modified high Cr ferritic steel employed in this experiment hinders the interface mobility for the shear-dominated martensitic transformation (the yield strength of this steel developed by our group is high to near 800 MPa at room temperature [38]); (2) the value of lengthening rate of martensitic lath is assumed as infinite, leading to the underestimation of the real velocity. Even so, the fitted values of v have the definite reliability of physical realness, which are compatible with those observed for pure iron ($\sim 3 \times 10^{-6}$ m/s[1]) [39] and Cu–Al–Ni alloy (about 10^{-6} to 10^{-2} m/s) [40]. Furthermore, the interface velocity for the massive γ(austenite) → α(ferrite) transformation as measured in pure Fe [41], Fe-2.96 % at. Ni [42], Fe-2.26 % at. Mn, and Fe-1.79 % at. Co [43] has been determined as in the range from 1.0×10^{-6} to 4.5×10^{-6} m/s, obviously approaching to the value for martensitic transformation in this work. The interface-controlled JMAK model has been developed to describe the kinetics of massive transformation. In the interface-controlled JMAK model, γ/α interface velocity is essential to γ → α transformation, of course unable to be considered as infinity. Similarly, it can be recognized that the growth rate of martensite (at least in the high Cr ferritic steels employed in this project) should not be regarded as infinity, and both the nucleation and growth for martensite would take effect on the course of transformation.

[1] Some claimed that so slow interface velocity may be due to the presence of carbon impurity (~0.03 wt%), and the measured value must be characteristic for the massive transformation in ultra-low carbon Fe-based alloy. Recent result also indicates that interface velocities with a martensitic nature in pure iron could reach values in the range of 200–700 m/s [18].

5 Conclusions

Kinetics of martensitic transformation in the high Cr ferritic creep-resistant steel upon various cooling rates was investigated by microstructural observation and high-resolution dilatometric measurements. A non-instantaneous growth model for martensitic transformation has been developed. Based on the experimental results and model analysis, it can be concluded as follows:

1. The proposed non-instantaneous growth model well describes the characteristics of athermal nucleation and non-instantaneous growth of martensite. The growth rate of martensite is found to be varied from 1×10^{-6} to 3×10^{-6} m/s. The so low mobility velocity of martensitic interface may be ascribed to the high strength of high Cr ferritic steel, and the assumption of infinite lengthening rate of martensitic lath.
2. Nucleation rate of martensite remains nearly the same irrespective of different cooling rates, which is compatible with the classic K–M equation and Magee model.
3. The growth rate of martensite can be accelerated by increasing cooling rate. Martensitic transformation would be promoted with the increase in cooling rate, since the nucleation rate is independent of the cooling rate.

Acknowledgments The authors are grateful to the China National Funds for Distinguished Young Scientists (Granted No. 51325401), the National Natural Science Foundation of China (Granted No. 51501126), the National Magnetic Confinement Fusion Energy Research Program (Granted No. 2015GB119001), and the Key Project of Natural Science Foundation of Tianjin (Granted No. 14JCZDJC38700) for Grant and financial support.

References

1. K. Kimura, Assessment of long-term creep strength and review of allowable stress of high Cr ferritic creep resistant steels, in *ASME 2005 Pressure Vessels and Piping Conference, American Society of Mechanical Engineers*, 2005, pp. 237–244
2. M. Taneike, F. Abe, K. Sawada, Creep-strengthening of steel at high temperatures using nano-sized carbonitride dispersions. Nature **424**, 294–296 (2003)
3. P. Ennis, A. Czyrska-Filemonowicz, Recent advances in creep-resistant steels for power plant applications. Sadhana **28**, 709–730 (2003)
4. K. Maruyama, K. Sawada, J.-I. Koike, Strengthening mechanisms of creep resistant tempered martensitic steel. ISIJ Int. (Japan) **41**, 641–653 (2001)
5. J.F. Salavy, L.V. Boccaccini, P. Chaudhuri, S. Cho, M. Enoeda, L.M. Giancarli, R.J. Kurtz, T.Y. Luo, K.B.S. Rao, C.P.C. Wong, Must we use ferritic steel in TBM? Fusion Eng. Des. **85**, 1896–1902 (2010)
6. Q. Huang, C. Li, Q. Wu, S. Liu, S. Gao, Z. Guo, Z. Yan, B. Huang, Y. Song, Z. Zhu, Y. Chen, X. Ling, Y. Wu, Progress in development of CLAM steel and fabrication of small TBM in China. J. Nucl. Mater. **417**, 85–88 (2011)
7. D.Y. Ku, S. Oh, M.-Y. Ahn, I.-K. Yu, D.-H. Kim, S. Cho, I.-S. Choi, K.-B. Kwon, TIG and HIP joining of reduced activation ferrite/martensitic steel for the Korean ITER–TBM. J. Nucl. Mater. **417**, 67–71 (2011)
8. Z. Nishiyama, *Martensitic transformation* (Elsevier, Amsterdam, 2012)
9. J. Yu, Q. Huang, F. Wan, Research and development on the China low activation martensitic steel (CLAM). J. Nucl. Mater. **367–370**, 97–101 (2007)
10. R. Lindau, A. Möslang, M. Schirra, P. Schlossmacher, M. Klimenkov, Mechanical and microstructural properties of a hipped RAFM ODS-steel. J. Nucl. Mater. **307**, 769–772 (2002)
11. S. Raju, B. Jeya Ganesh, A.K. Rai, R. Mythili, S. Saroja, E. Mohandas, M. Vijayalakshmi, K. Rao, B. Raj, Measurement of transformation temperatures and specific heat capacity of tungsten added reduced activation ferritic–martensitic steel. J. Nucl. Mater. **389**, 385–393 (2009)
12. B. Jeya Ganesh, S. Raju, A. Kumar Rai, E. Mohandas, M. Vijayalakshmi, K.B.S. Rao, B. Raj, Differential scanning calorimetry study of diffusional and martensitic phase transformations in some 9 wt% Cr low carbon ferritic steels. Mater. Sci. Technol. **27**, 500–512 (2011)
13. D. Koistinen, R. Marburger, A general equation prescribing the extent of the austenite-martensite transformation in pure iron-carbon alloys and plain carbon steels. Acta Metall. **7**, 59–60 (1959)
14. C. Magee, Nucleation of martensite. Pap. Ph. Transform. ASM **1970**, 115–156 (1970)
15. M. Grujicic, G. Olson, W. Owen, Mobility of martensitic interfaces. Metall. Trans. A **16**, 1713–1722 (1985)
16. Z.-Z. Yu, P.C. Clapp, Growth dynamics study of the martensitic transformation in Fe-30 pct Ni alloys: Part I. Quantitative measurements of growth velocity. Metall. Trans. A **20**, 1601–1615 (1989)
17. Y. Liu, L. Zhang, F. Sommer, E.J. Mittemeijer, Kinetics of martensite formation in substitutional Fe–Al alloys: dilatometric analysis. Metall. Mater. Trans. A **44**, 1430–1440 (2012)
18. C. Bos, J. Sietsma, B. Thijsse, Molecular dynamics simulation of interface dynamics during the fcc–bcc transformation of a martensitic nature. Phys. Rev. B **73**, 104117 (2006)
19. C. Liu, Y. Liu, D. Zhang, Z. Yan, Kinetics of isochronal austenization in modified high Cr ferritic heat-resistant steel. Appl. Phys. A **105**, 949–957 (2011)
20. C. Liu, D. Zhang, Y. Liu, Q. Wang, Z. Yan, Investigation on the precipitation behavior of M3C phase in T91 ferritic steels. Nucl. Eng. Des. **241**, 2411–2415 (2011)
21. C. Liu, Y. Liu, D. Zhang, Z. Yan, Research on splitting phenomenon of isochronal martensitic transformation in T91 ferritic steel. Phase Transitions **85**, 461–470 (2012)
22. Y. Liu, C. Liu, F. Sommer, E.J. Mittemeijer, Martensite formation kinetics of substitutional Fe-0.7 at.% Al alloy under uniaxial compressive stress. Acta Mater. **98**, 164–174 (2015)
23. S.M.C. van Bohemen, J. Sietsma, M.J.M. Hermans, I.M. Richardson, Kinetics of the martensitic transformation in low-alloy steel studied by means of acoustic emission. Acta Mater. **51**, 4183–4196 (2003)
24. D. McMurtrie, C. Magee, The average volume of martensite plates during transformation. Metall. Trans. **1**, 3185–3191 (1970)
25. C. Magee, H. Paxton, The Microplastic Response Of Partially Transformed Fe-31 Ni. Trans. Met. Soc. AIME **242**, 1741–1749 (1968)
26. J. Patel, M. Cohen, Criterion for the action of applied stress in the martensitic transformation. Acta Metall. **1**, 531–538 (1953)
27. J. Fisher, J. Hollomon, D. Turnbull, Kinetics of the austenite–martensite transformation. Trans. Am. Inst. Min. Metall. Eng. **185**, 691–700 (1949)
28. Q. Gao, Y. Liu, X. Di, L. Yu, Z. Yan, Martensite transformation in the modified high Cr ferritic heat-resistant steel during continuous cooling. J. Mater. Res. **27**, 2779–2789 (2012)
29. J.R.C. Guimarães, P.R. Rios, Initial nucleation kinetics of martensite transformation. J. Mater. Sci. **43**, 5206–5210 (2008)
30. J.R.C. Guimarães, P.R. Rios, Unified description of martensite microstructure and kinetics. J. Mater. Sci. **44**, 998–1005 (2009)
31. J.R.C. Guimarães, P.R. Rios, Martensite start temperature and the austenite grain-size. J. Mater. Sci. **45**, 1074–1077 (2010)
32. J.R.C. Guimarães, P.R. Rios, Modeling lath martensite transformation curve. Metall. Mater. Trans. A **44**, 2–4 (2012)
33. A. Entwisle, The kinetics of martensite formation in steel. Metall. Trans. **2**, 2395–2407 (1971)
34. F. Abe, Precipitate design for creep strengthening of 9 % Cr tempered martensitic steel for ultra-supercritical power plants. Sci. Technol. Adv. Mater. **9**, 013002 (2008)
35. J.R.C. Guimarães, P.R. Rios, Driving force and thermal activation in martensite kinetics. Metall. Mater. Trans. A **40**, 2264–2272 (2009)
36. H. Chen, S. Zwaag, Modeling of soft impingement effect during solid-state partitioning phase transformations in binary alloys. J. Mater. Sci. **46**, 1328–1336 (2010)
37. Y.H. Tan, C. De Zeng, X.C. Dong, Y.H. He, S.Q. Hu, New observation of martensitic morphology and substructure using transmission electron microscopy. Metall. Trans. A **23**, 1413–1421 (1992)
38. C. Liu, Y. Liu, B. Ning, Development of the modified high Cr ferritic heat-resistant steel. Mater. Res. Innovations **19**(S8), 813–818 (2015)
39. A. Gulyaev, M. Guzovskaya, Martensitic transformation in iron. Met. Sci. Heat Treat. **19**, 425–428 (1977)
40. M. Grujicic, G. Olson, W. Owen, Mobility of the β1-γ 1′ martensitic interface in Cu–Al–Ni: part I. Experimental measurements. Metall. Trans. A **16**, 1723–1734 (1985)
41. Y. Liu, F. Sommer, E. Mittemeijer, Abnormal austenite–ferrite transformation behaviour of pure iron. Phil. Mag. **84**, 1853–1876 (2004)
42. Y. Liu, F. Sommer, E. Mittemeijer, Austenite–ferrite transformation kinetics under uniaxial compressive stress in Fe-2.96 at.% Ni alloy. Acta Mater. **57**, 2858–2868 (2009)
43. Y. Liu, F. Sommer, E. Mittemeijer, Kinetics of the abnormal austenite–ferrite transformation behaviour in substitutional Fe-based alloys. Acta Mater. **52**, 2549–2560 (2004)